JOURNAL OF CATALYSIS 78, 306–318 (1982)

Sulfur on Noble Metal Catalyst Particles[1,2]

T. WANG,[3] A. VAZQUEZ, A. KATO,[4] AND L. D. SCHMIDT

Department of Chemical Engineering and Materials Science, University of Minnesota, Minneapolis, Minnesota 55455

Received February 25, 1982; revised July 2, 1982

The morphology and chemical composition of Pt, Rh, and Pd particles on amorphous SiO_2 were examined using X-ray photoelectron spectroscopy (XPS) and transmission electron microscopy (TEM) following their sequential treatment in H_2, H_2S, O_2, and SO_2. All metals form sulfides (PtS, Rh_2S_3, and PdS) readily upon heating in ~70 Torr of H_2S. XPS indicates that surface sulfidation is essentially complete by 300°C for metals, and TEM shows that 100-Å-diameter particles are completely converted to sulfide by 600°C. Considerable neutral sulfur is also formed on all metals. Treatment of sulfided particles in air produces oxides, sulfates, and metal. All sulfur is removed from Pd below 300°C to form PdO. Pt is converted mainly to PtO which decomposes to Pt metal above 450°C. Rh is converted to Rh_2O_3 and $Rh_2(SO_4)_3$ by 300°C, and some sulfate persists to above 500°C. Heating metals in SO_2 produces only sulfides for Rh and Pd, and sulfide, sulfate, and sulfur for Pt. Heating in an SO_2 and O_2 mixture produces sulfate on all metals. Rh particles exhibit evidence of melting when heated above 500°C in H_2S.

INTRODUCTION

The desirable properties of the Group VIII noble metal catalysts (*1*) are associated largely with their nobility (inertness toward compound formation in reactive gases) along with unfilled *d* electrons. Sulfur is the major common element which readily forms compounds with these metals, and most catalytic processes on them must take place at extremely low levels of sulfur contamination. These catalysts are sometimes regenerated by heating in O_2 to oxidize any sulfides to volatile SO_2 or SO_3. On the other hand, they are sometimes "presulfided" to reduce activity for undesired reactions.

The interactions of sulfur with noble metal catalysts is therefore an important issue in catalyst activity and stability. Properties of bulk sulfides are well known, but their sulfates are noncrystalline and poorly characterized. Since catalytic properties are associated with surface properties, surface rather than bulk structures determine behavior. Table 1 summarizes bulk oxides and sulfides of Pt, Rh, and Pd (*2, 3*). Pt and Rh sulfides are seen to be much more stable than oxides, although PdO is more stable than PdS.

Sulfur adsorption on macroscopic Pt (*4–6*) and Pd (*7*) surfaces has been characterized using a variety of surface analytical techniques, and its effect on adsorbates has been examined (*4*). The influence of sulfur on reactivities of noble metal catalysts has been studied by several investigators (*8–10*).

In this work we examine the morphologies, crystalline phases, and surface chemical composition and oxidation states of small particles of Pt, Rh, and Pd on amorphous SiO_2 following their treatment in H_2S, SO_2, O_2, and H_2. The combination of transmission electron microscopy (TEM) and X-ray photoelectron spectroscopy

[1] This work was partially supported by NSF under Grant CPE8017440.

[2] Surface analysis was through the NSF Regional Instrumentation Facility for Surface Analysis at the University of Minnesota, and electron microscopy was through the Electron Microscopy Center.

[3] Present address: Shell Oil Company, Houston, Tex.

[4] Present address: Hitachi Research Laboratory, Ibari-ken, Japan.

0021-9517/82/120306-13$02.00/0

TABLE 1

Properties of Metal Oxides and Sulfides[a]

Metal	Oxide	T_d[b] (°C)	Sulfide	T_d[b] (°C)
Pt	PtO_2(orth)	450	PtS_2(hex)	350
	PtO(tetrag)	507	PtS(tetrag)	800
Rh	Rh_2O_3(orth)	1100	Rh_2S_3(orth)	1900
	RhO_2(tetrag)	1400	RhS_2(cubic)	—
Pd	PdO(tetrag)	870	PdS(tetrag)	600

[a] Data taken from Refs. (*2, 3*).

[b] Decomposition temperatures in O_2 at 1 atm or in $P_{H_2} = P_{H_2S}$.

(XPS) on the same samples provides definitive and semiquantitative information about these systems, although obviously many aspects remain to be elucidated. The results and their interpretation will be presented together, and in the Discussion and Summary we shall attempt to generalize the processes involved and speculate on how they might interpret catalyst morphological changes.

EXPERIMENTAL

The apparatus and procedures are similar to those described in studies of oxidation and reduction of these metals (*11, 12*). Metal particles approximately ~100 Å in diameter were prepared by vacuum depositing ~10-Å films of metal on planar amorphous SiO_2 and heating in H_2 to 600°C. The SiO_2 was prepared by air oxidizing high-purity Si(111) wafers to form 1000-Å amorphous SiO_2 films over their surfaces. For XPS a 5 × 5-mm area was examined, and TEM images were obtained through a 500-Å flake of SiO_2 placed over a hole in the wafer. In most experiments different but identically prepared samples were used for XPS and TEM to avoid contamination during examination.

Samples were heated for 2 h in high-purity flowing gases at a pressure of 1 atm in a heated quartz tube. Except where noted, the same sample was examined sequentially following various gas and temperature treatments. Tests were repeated on several samples with all results consistent with those shown here.

A JEOL JEM100CX with 3.5-Å resolution was used for TEM and a Perkin–Elmer physical electronics model 555 was used for XPS. Most XPS spectra were acquired in approximately 20 min for a peak resolution of 1.2 eV. Relative amounts of elements were obtained from peak areas using published sensitivity calibrations (*12*) without corrections for depth sensitivities. Peak energies were calibrated against the Si(2*p*) peak at 103.4 eV. Sample charging was never more than 2 eV. After correction the relative peak positions for all elements on all samples were within 0.2 eV of published values and calibrations obtained in this laboratory on metals and metal oxides. Oxidation states of sulfur were obtained by computer deconvolution of the S(2*p*) states using published peak positions (*13*) for sulfide, elemental sulfur, and sulfate.

SULFIDATION OF METAL PARTICLES

Figure 1 shows typical XPS survey spectra of SiO_2 and of Pt particles on SiO_2 following treatment in 10% H_2S in N_2 at 1 atm

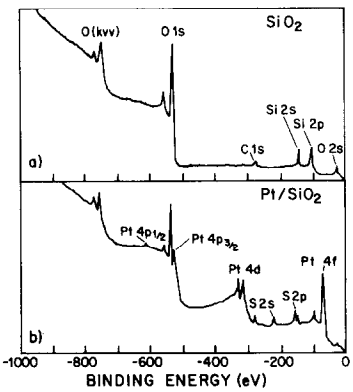

FIG. 1. Typical XPS survey spectra of (a) planar amorphous SiO_2 and (b) the same sample after vacuum deposition of 10 Å of Pt. Both samples were heated in 10% H_2S in N_2 at 1 atm for 2 h at 600°C. No contamination is observed on either sample except for traces of carbon. The S(2*p*), O(1*s*), and Pt(4*f*) lines are shown at higher resolution in following figures for various heat and gas treatments.

at 600°C. No sulfur is deposited on SiO_2 alone by this treatment, and all peaks can be identified as XPS or X-ray Auger lines of Si and O. However, with Pt on SiO_2 the sulfur $2s$ and $2p$ peaks are evident along with the Pt($3d$) and Pt($4f$) peaks. This shows that no sulfur is deposited on SiO_2 by H_2S exposure at these temperatures, and therefore the sulfur is associated exclusively with metal particles. The only contaminant observed in any XPS spectrum was carbon. We believe that carbon is introduced in transfer between the reactor and the XPS instrument because the carbon peak was typically a monolayer (referenced to CO saturation coverage on clean Pt) and it exhibited no systematic variations with heat or gas treatment. In all succeeding figures we shall show only high-resolution XPS spectra of S, O, and metals.

Figures 2, 3, and 4 show the O($1s$), S($2p$), and metal lines for Pt, Rh, and Pd, respectively. The vertical lines are at energies corresponding to O($1s$) from SiO_2 at 532.6 eV, the S($2p$) line of elemental sulfur at 164.0 eV, the Pt($4f_{7/2}$) line of metallic Pt at 70.9 eV, the Rh($3d_{5/2}$) line of metallic Rh at 307.0 eV, and the Pd($3d_{5/2}$) line of metallic Pd at 334.5 eV.

Sulfidation begins upon exposure to H_2S at 25°C for all metals, and sulfur peak areas reach their ultimate values at ~300°C. Figure 5 shows a plot of S($2p$)/M ratios for all three metals. It is evident that the major S peak is that of sulfide (S^{2-}) with considerable neutral S forming at higher temperatures. Metal peaks shift upon sulfidation with shifts yielding Pt^{2+}, Rh^{3+}, and Pd^{2+}, respectively. Figure 6 shows a plot of measured metal peak shifts versus treatment, gas, and temperature. While little literature exists on metal peak positions for these sulfides, all are close to those of the corresponding oxides of these valences. Some double metal peaks are observed for situations where both metal and cation appear to exist, but shifts were too small for accurate curve fitting.

For Rh and Pd samples, small O($1s$) peaks at a lower binding energy than that of O($1s$) from SiO_2 are observed after treatment at 25°C; these arise from monolayer amounts of Rh_2O_3 and PdO which form upon room-temperature exposure of the metals to air as noted previously (*11*). The O($1s$) peaks do not appear on the sulfided particles; this shows that the metal sulfides do not pick up oxygen upon low-tempera-

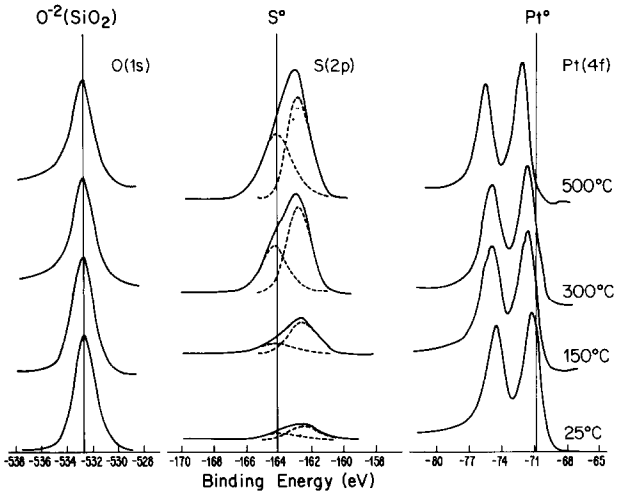

FIG. 2. XPS spectra of O, S, and Pt following treatment in 10% H_2S for 2 h at increasing temperatures shown in the figure. Sulfide and sulfur (vertical line at 164.0 eV) are observed and Pt metal (vertical line at 70.8 eV) is converted to Pt^{2+} (72.2 eV) by this treatment.

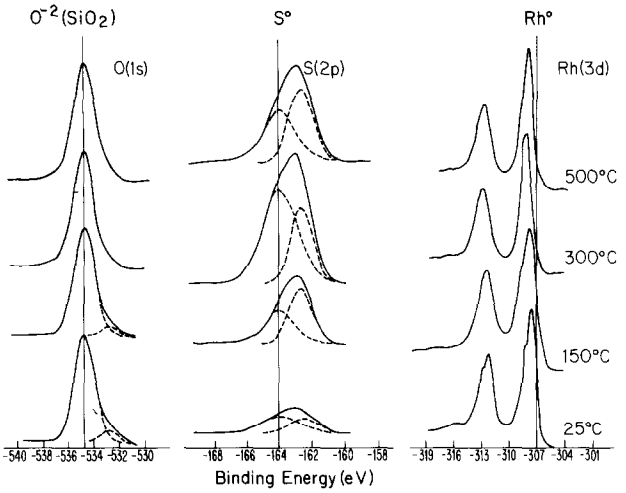

FIG. 3. XPS spectra of O, S, and Rh metal following treatment in 10% H_2S for 2 h at increasing temperatures shown in the figure. Sulfide and sulfur (vertical line at 164.0 eV) are observed and Rh metal (vertical line at 307.0 eV) is converted to Rh^{3+} (308.1 eV) by this treatment.

ture exposure to air. The measured S/M atomic ratios of Fig. 5 (1.0 for Pt, 2.0 for Rh, and 1.0 for Pd) are fairly close to the stoichiometries expected for the most stable sulfides, PtS, Rh_2S_3, and PdS, although neutral sulfur is included in measured ratios. Also, the metal peak positions show that all metal is ionized with charges expected for these compounds. Therefore, we conclude that, upon treatment in H_2S, at least the top 10–20 Å (the nominal depth sensitivity of XPS) of all particles is converted completely to sulfides with these valences and approximately these stoichiometries.

AIR TREATMENT OF SULFIDED METALS

Figures 7, 8, and 9 show O(1*s*), S(2*p*), and metal XPS peaks after heating the sulfided metals (Figs. 2–4) in air at succes-

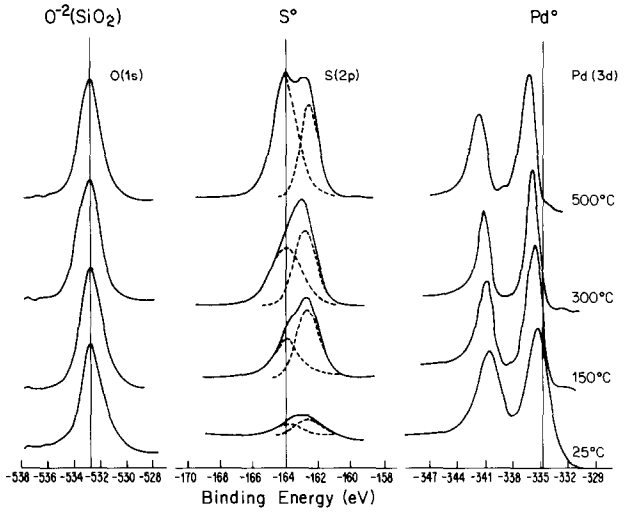

FIG. 4. XPS spectra of O, S, and Pd following treatment in 10% H_2S for 2 h at increasing temperatures shown in the figure. Sulfide and sulfur (vertical line at 164.0 eV) are observed and Pd metal (vertical line at 334.9 eV) is converted to Pd^{2+} (336.5 eV) by this treatment.

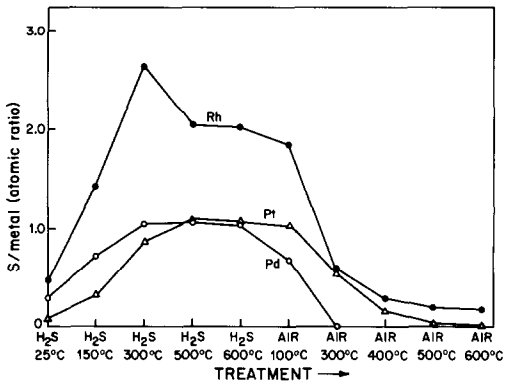

FIG. 5. Plot of sulfur-to-metal atomic ratio (obtained from XPS peak areas) versus treatment in H_2S and then air at temperatures shown. Data are taken from spectra of Figs. 2 through 4 and 7 through 9.

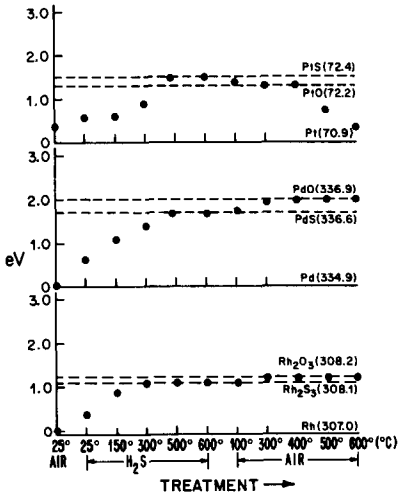

FIG. 6. Plot of metal XPS peak positions versus treatment in H_2S and then air at temperatures shown. Data are taken from Figs. 2 through 4 and 7 through 9.

sively higher temperatures indicated in the figures.

After heating to 100°C only slight changes are noted, but by 300°C large changes in S and O peaks are evident. For Pt the sulfur decreases noticeably at 300°C and almost completely disappears by 500°C. For Rh, S^{2-} is replaced by S^{6+} by 300°C, and for Pd all sulfur has disappeared by 300°C.

Figures 5 and 6 summarize the S/M peak area ratios and metal peak positions after heating sulfided metals in air at temperatures shown. It is evident that sulfur disappears rapidly on Pd but remains to above 500°C on Rh. Chemical shifts show that Rh_2S_3 transforms to Rh_2O_3 and $Rh_2(SO_4)_3$ upon heating in air and that PtS transforms to $PtSO_4$ and PtO at low temperatures. We do not observe any $PdSO_4$ except by heating in air an SO_2 and O_2 mixture as described in the next section.

After treatment of the sulfided particles in air, all metals exhibit O(1*s*) XPS lines at

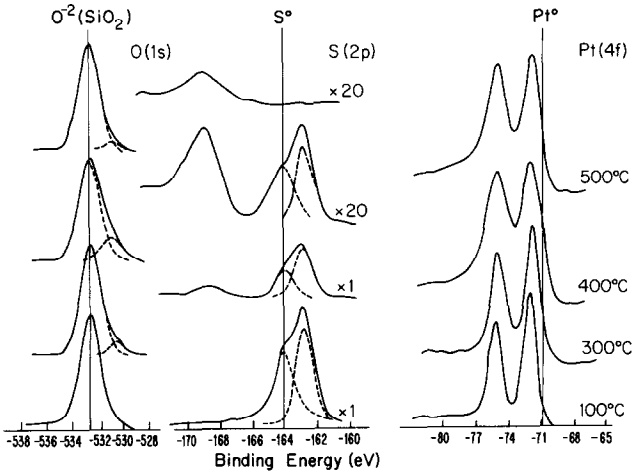

FIG. 7. XPS spectra of O, S, and Pt following treatment of sulfided particles in air at temperatures shown. PtO and $PtSO_4$ are observed to form as sulfide is removed.

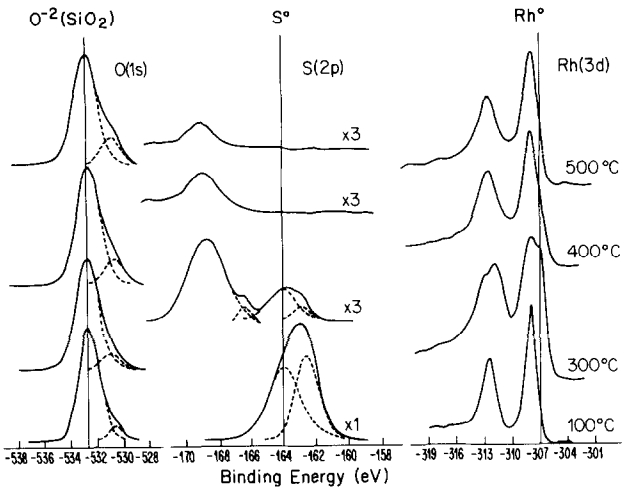

FIG. 8. XPS spectra of O, S, and Rh following treatment of sulfided particles in air at temperatures shown. Rh_2O_3 and $Rh_2(SO_4)_3$ are observed to form as sulfide is removed.

~530 eV which are characteristic of metal oxides as shown in Figs. 7–9. The O(1*s*) lines of metal sulfates (*12*) occur at ~532 eV which causes the peak to be undetectable because it occurs at the same energy as O(1*s*) from SiO_2. The peak identified as metal oxide also does not correlate with the S^{6+} peak as would be expected if it were a sulfate. The formation of this O(1*s*) peak and the disappearance of sulfur on Pd and Pt show that these metals are transformed from sulfides to oxides by this treatment.

Relative amounts of sulfide, oxide, sulfate, and metal were estimated from XPS peak areas and positions as shown in Table 2. The sulfate-to-sulfide ratio was obtained from the S^{6+}/S^{2-} area ratio, and the metal-to-cation ratio was obtained assuming a linear shift in peak position with amount oxidized. The amount of oxide was obtained from the O(1*s*) peak area at 530 eV, assuming that sulfate and silica gave O(1*s*) signals at ~532 eV. Percentages were generally consistent between methods, but values in

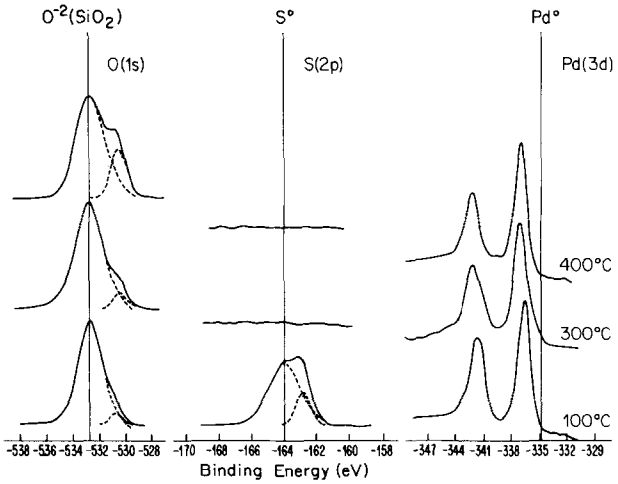

FIG. 9. XPS spectra of O, S, and Pd following treatment of sulfided particles in air at temperatures shown. All sulfur is removed by 300°C and particles are converted entirely to PdO.

TABLE 2

Composition of Sulfided Particle Surfaces following Air Treatment

Metal	Compound	Percentage metal at:		
		300°C	400°C	500°C
Pt	$PtSO_4$	9	8	7
	PtS	29	5	0
	PtO	41	82	25
	Pt	20	5	68
Rh	$Rh_2(SO_4)_3$	14	20	15
	Rh_2S_3	1	0	0
	Rh_2O_3	58	80	85
	Rh	27	0	0
Pd	$PdSO_4$	0	0	0
	PdS	0	0	0
	PdO	96	100	100
	Pd	4	0	0

Table 2 should be taken only as rough estimates of amounts of phases present. No corrections were made for metal dilution in compound formation, sensitivity variations with depth, backscattering variations, etc.

However, it seems clear from inspection of Table 2 and from the spectra that sulfates are formed on Rh and Pt while none occurs on Pd. Also, upon treatment of sulfides in air, Rh metal is formed at ~300°C and Pt metal is formed above 500°C; oxygen can also cause a reduction of the Rh as will be discussed later.

SULFUR DIOXIDE TREATMENT OF METALS

A series of experiments was conducted in which the reduced metals were heated in 10% SO_2 in N_2 and in 10% SO_2 in air.

Sulfur dioxide alone at 500°C (Fig. 10) produced sulfide and neutral sulfur on all three metals with some sulfate observed on Pt. Chemical shifts of metals are again characteristic of Pt^{2+}, Rh^{3+}, and Pd^{2+}. Oxidation states of metals and sulfur are nearly indistinguishable from those observed after treatment in H_2S alone.

When metals are heated to 500°C in a mixture of SO_2 and O_2 (Fig. 11), the metal oxidation states are unchanged but the oxidation state of sulfur now is primarily S^{6+}. This shows that metals are converted to sulfates by heating in an SO_2 and O_2 mixture. Figure 11 shows that Pd is converted mostly to PdO with some $PdSO_4$. This treatment causes Pt to transform largely to $PtSO_4$.

PARTICLE MORPHOLOGIES

Particles were examined by TEM at vari-

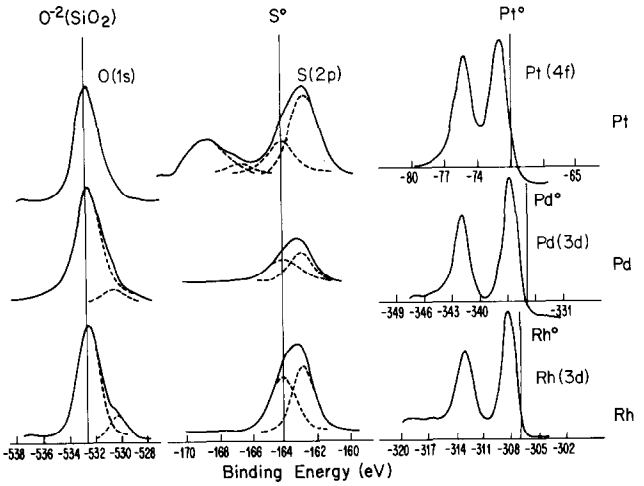

FIG. 10. XPS spectra of O, S, and metals following treatment of metal particles in SO_2 at 500°C. On Rh and Pd sulfide and sulfur are observed while Pt also forms sulfate.

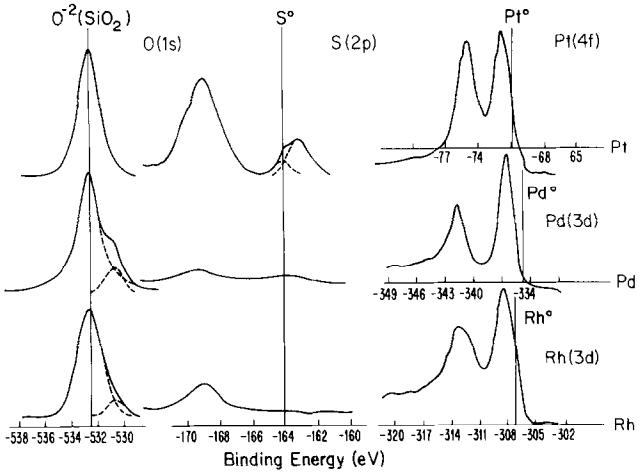

FIG. 11. XPS spectra of O, S, and metals following treatment of metal particles in a 10% SO_2, 90% O_2 mixture at 500°C. Sulfur is present mainly as sulfate on Pt and Rh while Pd is converted mostly to PdO.

ous stages of sulfidation, oxidation, and reduction. Bright-field imaging, electron diffraction, and dark-field imaging were used to determine morphologies and relative amounts and locations of crystalline phases.

Figure 12 shows a sulfidation sequence for Pt particles. Figure 12a shows the original sample after annealing in H_2 at 600°C, Figs. 12b–d are following H_2S treatment at 300, 500, and 600°C, respectively, while Fig. 12e is after air oxidation of the sulfided particles at 300°C. Treatment of Pt in H_2S causes particles to expand parallel to the surface. The flat facets which are typical of metal are also transformed into irregularly shaped edges, and small crystallites appear to form near the edges of the original particle. Electron diffraction showed that tetragonal PtS was first detected after heating to 300°C, and complete transformation to sulfide (no fcc lines) occurred at 600°C. Figure 12f shows the electron diffraction pattern of the sample from Fig. 12c. All diffraction lines can be identified with tetragonal PtS; no fcc metal or hexagonal PtS_2 lines were observed. Several nearby pairs of particles are also observed to be pulled closer together upon sulfidation below 500°C. We observed a similar low-temperature process upon oxidation of Ir (*10*). Evidently the formation of a compound "bridge" between particles produces a force which draws them together, but we have no detailed explanation for this effect.

Figure 13 is a similar sequence of micrographs showing sulfidation of Rh particles. Figure 13a shows Rh metal particles after heating in H_2 at 600°C; only fcc diffraction lines are observed. Figures 13b, c, and d show the same particles after heating in 10% H_2S. At 300°C particle cores retain their metallic character with the same twin configurations as in Fig. 13a. However, all particles are surrounded by a lower-contrast shell of Rh_2S_3 between 10 and 30 Å wide. After heating to 500°C (Fig. 13c) the particles appear more ragged, although many of the original metal twins are still evident. Electron diffraction indicates both metal and Rh_2S_3 are present at 500°C.

After heating to 600°C the sulfided particles have distinctly different morphologies, and electron diffraction indicates Rh_2S_3 as the major crystalline phase (Fig. 13d). Several faint lines were observed upon high-temperature sulfidation which indicates traces of another phase, probably another sulfide (*3*). Several low-contrast particles 30 to 100 Å in diameter grow from each parent particle. These particles have distinct curved edges, and boundaries between

parent and daughter particles are also quite sharp. We suggest that the structures formed by sulfiding Rh_2S_3 above 500°C indicate melting of the particles as will be discussed later.

Figure 13e shows the same sulfided particles after heating in air at 300°C. Particles now appear visually to be more crystalline than sulfides, with multiple twins occurring frequently. However, particle outlines are less distinct than those for sulfided particles. Electron diffraction of this surface

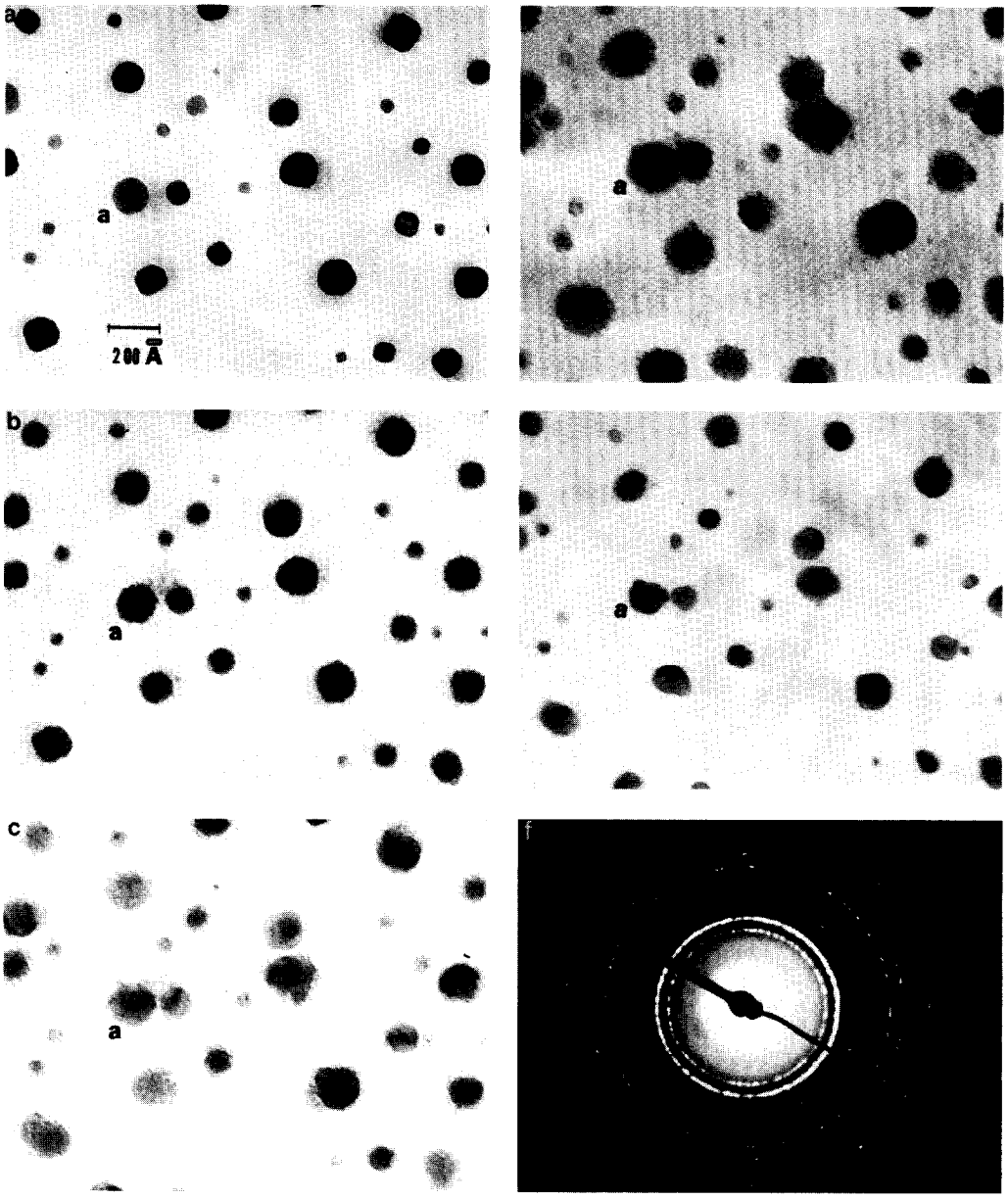

FIG. 12. Electron micrographs of Pt particles on planar SiO_2 following sequential heat treatments in H_2S and then air: (a) after heating in H_2 at 600°C to form metal particles; (b) after heating (a) in H_2S at 300°C; (c) after heating (a) in H_2S at 500°C; (d) after heating (a) in H_2S at 600°C; (e) oxidized in air at 300°C; (f) electron diffraction pattern of PtS corresponding to micrograph (d). The letter "a" indicates the identical location on each micrograph.

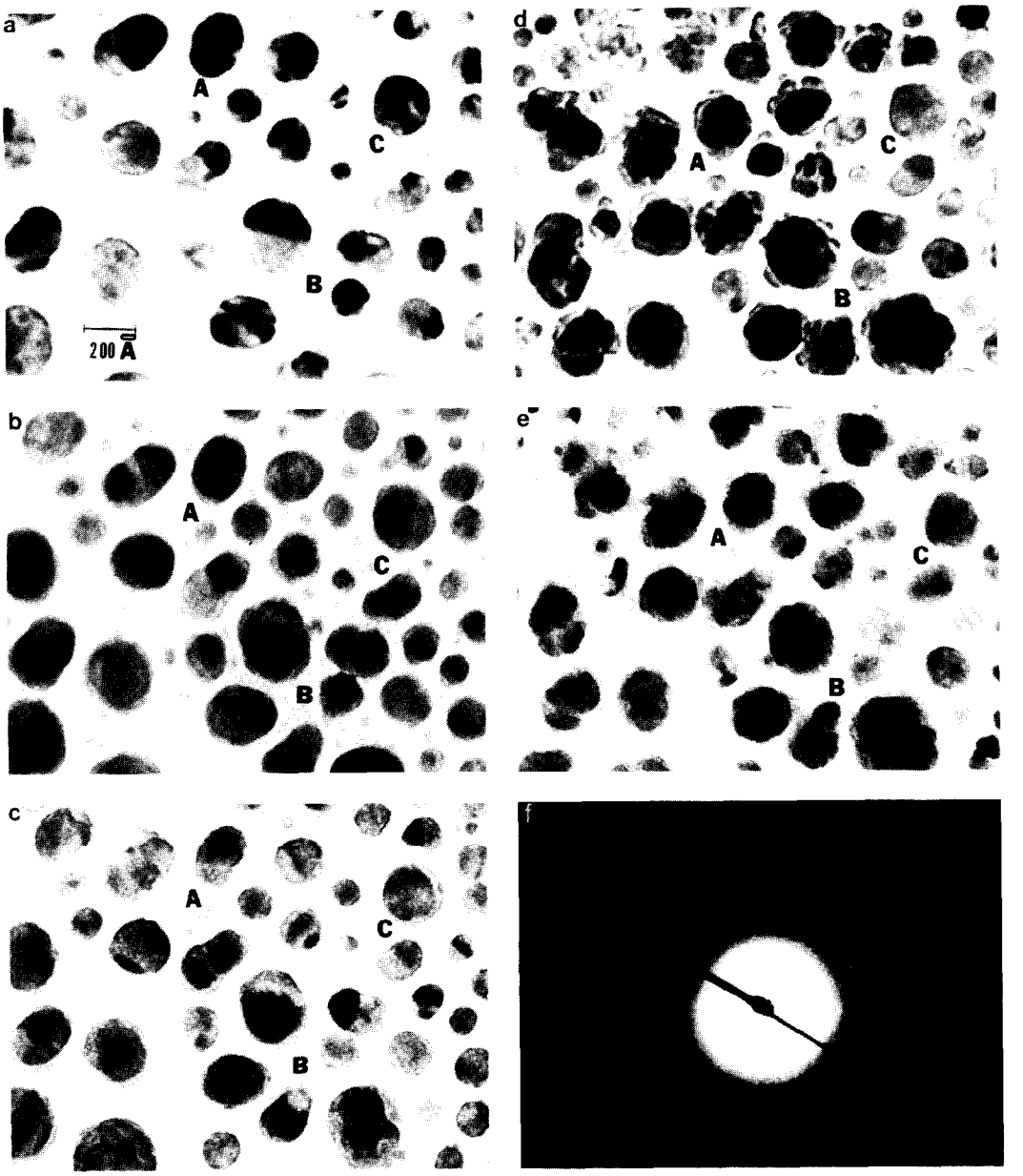

FIG. 13. Electron micrographs of Rh particles on planar SiO_2 following sequential heat treatments in H_2S and then air: (a) after heating in H_2 at 600°C to form metal particles; (b) after heating in H_2S at 300°C; (c) after heating in H_2S at 500°C; (d) after heating in H_2S at 600°C; (e) oxidized in air at 300°C; (f) electron diffraction pattern of Rh_2S_3 corresponding to micrograph (d). Letters "A, B, and C" indicate locations on each micrograph.

gave lines characteristic of a mixture of Rh_2O_3 and Rh_2S_3.

HEATING IN Cl_2

Several experiments were carried out in which Pt particles were heated in 1% Cl_2 in N_2. Complete loss of Pt occurred if heated above 100°C. At −75°C we observed only Pt^{2+} along with Cl^- XPS lines, indicating that solid $PtCl_2$ can be formed at low temperatures. However, the chlorides are sufficiently volatile that they evaporate at low

temperatures and are thus difficult to study on planar substrates. Chlorine is more effective than sulfur in oxidizing these metals, but formation of volatile products interferes with experiments comparable to those using sulfur.

DISCUSSION

Reactions

Sulfides and neutral sulfur readily form on all of these metals when they are heated in H_2S. These transformations can be regarded as the reactions

$$M + xH_2S \rightarrow MS_x + xH_2 \quad (1)$$

and

$$H_2S \xrightarrow{M} S + H_2. \quad (2)$$

Sulfide and sulfur are detected at room temperature, surface sulfidation is complete at ~300°C, and 100-Å particles are completely converted to sulfide by 500°C. A single crystalline sulfide and a single metal oxidation state are observed on each metal.

Treatment of the sulfides in air produces oxides, sulfates, and metal. These transformations can be written as the reactions

$$MS_x + (3x/2)\,O_2 \rightarrow MO_x + xSO_2, \quad (3)$$

$$MS_x + 2xO_2 \rightarrow M(SO_4)_x, \quad (4)$$

and

$$MS_x + xO_2 \rightarrow M + xSO_2. \quad (5)$$

PdS is transformed completely to oxide, while Rh_2S_3 and PtS are transformed to oxide and sulfate.

While reactions (3) and (4) represent oxidation of sulfur from S^{2-} to S^{4+} and S^{6+}, respectively, reaction (5) represents reduction of Rh^{3+} to Rh^0 (Fig. 8, 300°C in air) and of Pt^{2+} to Pt^0 (500°C in air). In the case of Rh oxygen evidently oxidizes the sulfide (perhaps to sulfate) which reduces Rh^{3+} ions in a solid-state reaction (probably forming volatile SO_2).

Formation of PtO by reaction (3) produces a surface phase rather than the more stable PtO_2. Surface oxides of Pt have been a subject of active investigation with little consensus of data from electrochemistry, gas exposure, and catalysis. In the present situation we believe we form PtO by ionization of Pt^0 by H_2S to Pt^{2+} followed by replacement of S^{2-} by O^{2-} in the lattice. We observe a similar process in Pt foils. We shall describe these experiments and their interpretation in a later paper.

None of these results appears to be inconsistent with literature values of thermodynamic properties (*2, 3*) in that no phases are stable above their decomposition temperatures as listed in Table 1. Sulfate should not be stable (reaction (4)) compared to oxide (reaction (3)) since no gaseous form of sulfur is available to stabilize the sulfates. Sulfate must therefore be formed by a solid-state reaction of O_2 with MS_x. It should also be noted that SO_2 alone is not a particularly efficient way to make sulfate (Fig. 10). On all metals, the metal is transformed mainly to sulfide by heating in SO_2. The process may be written as

$$M + 3xSO_2 \rightarrow MS_x + 2xSO_3$$

or a similar reaction which reduces S^{4+} to S^{2-}.

In contrast to SO_2 alone, a mixture of SO_2 and O_2 readily produces sulfates on Rh and Pt but mostly forms oxide on Pd (Fig. 11). These metals are excellent catalysts for SO_2 oxidation; this gas mixture should therefore become a source of SO_3 for sulfate formation.

Comparison of Morphologies of Sulfide, Oxide, and Sulfate

Oxides on Rh and Pd are completely crystalline (*9*) at all temperatures. On Rh particles the oxide forms as a film of rather uniform thickness over the metals below 500°C, while crystals nucleate and grow above this temperature. Pt forms no detectable oxide by heating in air at 1 atm.

Sulfides form at comparable or lower temperatures than do oxides, and sulfides are also at least partially crystalline. Both

oxides and sulfides are observed to spread over the SiO_2 upon heating to high temperatures.

Morphologies of sulfides and oxides appear microscopically to be quite different. Sulfides seem to form smaller crystallites than do oxides as seen by dark-field imaging of the respective compounds. While some sulfide is always observed by electron diffraction, it is possible that amorphous sulfide also exists. Sulfide is always accompanied by neutral sulfur which is presumably amorphous. The morphological differences may therefore be associated with the sulfur phase. It should be noted that a sulfur phase should be nearly invisible in electron microscopy because electron scattering from sulfur is very weak compared to that from the higher-atomic-number metals.

Sulfate morphologies are more difficult to characterize because they are completely noncrystalline and are detectable only by the S^{6+} XPS line. Also, sulfate always occurs along with oxide and/or sulfide which makes identification even more difficult.

The distinctly different morphologies of oxide compared with sulfide or sulfate may thus arise from the poorer crystallinity of the latter or because they occur in the presence of multiple phases. The nucleation and growth processes of the different phases could also be quite different even if thermodynamic properties were comparable.

Particle Melting

When Rh_2S_3 is heated above 500°C, a distinctive morphology is observed (Fig. 12d) which we have never observed after heating Pt, Rh, Pd, or Ir in air (*9*) or in H_2S. The multiple particles emanating from each parent crystallite with sharp but curved outlines have an appearance which one would expect if a liquid phase had existed. Such morphologies appear to be unique in the transformations of small particles. The oxides all decompose far below their melting points (*2*), and none of the Rh sulfides is reported to have a low melting point (*3*).

Thus, we believe that in all situations except that for Rh_2S_3 above 500°C all processes are consistent with solid-state transformations. All observations of Rh_2S_3 particles suggest that Rh_2S_3 melts between 500 and 600°C. It should be noted that sulfur and metal are present, and these could form a eutectic which melts below the melting points of any pure components. We only identify Rh^{3+} compounds in XPS while RhS_2 is also reported to exist. Because of the Rh(3*d*) doublet in XPS, it is difficult to identify small amounts of another state so that some mixed-valence compounds of Rh may also be present in the sulfide.

There has been considerable speculation in the literature regarding the possibility of particle melting (mostly for metals) with the main evidence for this being a high mobility of particles above a certain temperature (the Tamman temperature). However, we (*1*) have never observed any particle motion on SiO_2 or Al_2O_3 supports except when phase transformations are taking place, and we regard atomic migration as the only important mechanism of metal particle sintering, at least on these supports.

We suggest that either Rh_2S_3 or a eutectic mixture melts and forms several blobs of liquid from each original particle. Examination of Fig. 13 and other micrographs of this system shows that only some particles melt. A variable melting point would be expected from a mixture because of composition variations between particles.

Reaction exothermicity should not be significant in causing melting because the rate of heat generation in solid-state transformations is slow, and only the SO_2 and O_2 system could generate sufficient reaction heat to increase particle temperatures.

SUMMARY

Even relatively simple systems of noble metals on planar silica supports exhibit compositions and morphologies in reactive gases which are quite complex. The structures formed depend strongly on the temperature–time–gas history of the system in ways that appear to be unpredictable from

thermodynamic data or intuition. For real high-area supported oxide catalysts, the complications of additional species and the multiple-step preparation and calcining processes should be expected to produce structures much more complex than those observed here.

Nevertheless, relative thermodynamic stabilities appear to correlate qualitative features of phases observed in metals, oxides, sulfides, and sulfates. Transformation processes in formation of oxides and sulfides seem to follow a film growth mechanism at low temperatures, crystallite nucleation and growth at higher temperatures, and spreading over the substrate at even higher temperatures. These are roughly as intuition would predict.

Transformations associated with melting have seldom been observed with pure systems, and they may be associated with decreased and variable melting points of particles having multiple phases present simultaneously. This situation should be expected more commonly with real catalysts than with simplified laboratory prototypes.

Finally, we note that transformations of catalyst particles should in general be significant in determining the surface properties of supported catalysts. Surface areas, elements present at the surface, surface phases, crystal planes, and surface defects should clearly depend upon treatment conditions. Such phenomena are certainly responsible for some instances of poor reproducibility of catalyst properties. In a later publication we shall describe more detailed electron microscopy of microstructures in the Rh system in the presence of H_2S and air.

REFERENCES

1. Anderson, J. R., "Structure of Metallic Catalysts." Academic Press, New York, 1975.
2. Samsonov, G. V., "The Oxide Handbook," p. 164. IFI/Plenum, New York, 1973.
3. Millers, K. C., "Thermodynamic Data for Inorganic Sulfides, Selenides, and Tellurides." Butterworths, London, 1974.
4. Fischer, T. E., and Keleman, S. R., *J. Catal.* **53,** 24 (1978).
5. Bonzel, H. P., and Ku, R., *J. Chem. Phys.* **58,** 4617 (1973); **59,** 1641 (1973).
6. Berthier, T., Perdereau, M., and Oudar, J., *Surf. Sci.* **36,** 225 (1973).
7. Matsumoto, Y., Onishi, T., and Tamaru, K., *J. Chem. Soc. Faraday Trans. 1* **76,** 1116, 1122 (1980).
8. Summers, J. C., and Baron, K., *J. Catal.* **57,** 380 (1979).
9. Tsai, J., Agrawal, P. K., Foley, J. M., Katzer, J. R., and Manogue, W. H., *J. Catal.* **61,** 192 (1980); Tsai, J., Agrawal, P. K., Sullivan, D. R., Katzer, J. R., and Manogue, W. H., *J. Catal.* **61,** 204 (1980).
10. Fuentes, S., and Figueras, F., *J. Catal.* **54,** 397 (1978).
11. Wang, T., and Schmidt, L. D., *J. Catal.* **70,** 187 (1981); **66,** 301 (1980).
12. Wang, T., and Schmidt, L. D., *J. Catal.* **71,** 411 (1981).
13. Mullenberg, G. E., (Ed.), "Handbook of X-Ray Photoelectron Spectroscopy." Perkin–Elmer Press, 1978.